Electrical resistivity of CuAlMo thin films grown at room temperature by dc magnetron sputtering

Martin Birkett* and Roger Penlington

Faculty of Engineering and Environment, Northumbria University,

Ellison Building, Newcastle upon Tyne, NE1 8ST, UK.

*Tel: +44 191 227 3763 martin.birkett@northumbria.ac.uk

Abstract

We report on the thickness dependence of electrical resistivity of CuAlMo films grown by dc magnetron sputtering on glass substrates at room temperature. The electrical resistance of the films was monitored in situ during their growth in the thickness range 10-1000 nm. By theoretically modelling the evolution of resistivity during growth we were able to gain an insight into the dominant electrical conduction mechanisms with increasing film thickness. For thicknesses in the range 10-25 nm the electrical resistivity is found to be a function of the film surface roughness and is well described by Namba's model. For thicknesses of 25-40 nm the experimental data was most accurately fitted using the Mayadas and Shatkes model which accounts for grain boundary scattering of the conduction electrons. Beyond 40 nm, the thickness of the film was found to be controlling factor and the Fuchs-Sonheimer model was used to fit the experimental data, with diffuse scattering of the conduction electrons at the two film surfaces. By combining the Fuchs and Namba models a suitable correlation between theoretical and experimental resistivity can be achieved across the full CuAlMo film thickness range of 10-1000 nm. The irreversibility of resistance for films of thickness >200 nm, which demonstrated bulk conductivity, was measured to be less than 0.03 % following subjection to temperature cycles of -55 and +125 ºC and the temperature co-efficient of resistance was less than ±15 ppm/ºC.

Keywords: Resistivity; thin film; CuAlMo.

1. Introduction

The ternary system of copper–aluminium–molybdenum (CuAlMo) has recently been reported to show promise in the preparation of thin film resistive materials due to its excellent long-term stability and low temperature coefficient of resistance [1-3]. Work to date on this metal alloy has focussed on studying the effect of varying deposition process conditions on structural and electrical properties and relating them to fundamental theories regarding the condensation mechanism of the thin films onto the substrate. Work in this current paper will deal with the effect of the CuAlMo film thickness on its physical properties, with particular attention being given to electrical resistivity.

It is often convenient to categorise thin films used in the manufacture of resistors by the electrical conduction mechanisms present. For thin films of conducting materials, such as metals, alloys and semiconductors, the main differences in their physical properties when compared with their bulk counterpart are due to the thinness of the film and also the preparation process and conditions.

The dominant electrical conduction mechanism is strongly dependant on the degree of thinness of the film, which is usually categorized by two distinct stages of growth; discontinuous and continuous. During the early stages of growth the film consists of small nucleation islands separated from each other by small distances of 0.1-10 nm. This type of film is called a discontinuous or island film. The electrical properties of such a film are very different to the properties of a bulk metal and behaviour is closer to that of a semiconductor, the resistivity often being many orders of magnitude higher. The conduction in a discontinuous film is basically a function of the spaces between the islands, across which electrons must jump to enable an electric current to flow, the resistance of the islands themselves being insignificant in comparison.

As the deposition process continues, these islands increase in size and eventually become so large that they join to form a continuous film, showing metallic type conductivity. The thickness at which this phenomenon occurs is deemed the critical thickness, h_{cr}.

For film thicknesses beyond h_{cr} the metal film is continuous and the main contribution to the total resistance is from the resistance of the grains themselves. The resistance of the film decreases by around an order of magnitude in this transition from an island structure to a continuous film.

A typical example of the dependence of resistivity on film thickness is shown for aluminium films grown on glass substrates at various condensation temperatures [4]. The critical thickness increases from approximately 3 to 7 nm with increase in condensation temperature from 25 to 120ºC. This can be explained by the increase in mobility of the adsorbed atoms with temperature, which form fewer but larger nucleation sites or islands. Therefore the film will be thicker at the point at which these islands join together; the critical thickness [5]. If the thickness of a film is comparable with the mean free path (MFP) of the bulk material, the boundaries of the film impose a geometric restriction on the movement of the conduction electrons, through scattering, and therefore on the real MFP of the carriers, resulting in a decrease in conductivity of the metal film compared with that of the bulk material.

This scattering of conduction electrons at the film surfaces is the so called size effect and it was first predicated in a widely cited theoretical paper by K. Fuchs [6] in 1938 that the electrical resistivity of thin metal films increases with decreasing thickness. Due to good agreement with experimental data, Fuchs' theory was not called into question for a significant period. However it later became obvious that in addition to surface scattering, grain boundary scattering [7] and surface roughness contributions [8] also have a significant effect on the resistivity behaviour of polycrystalline films.

This paper considers some aspects of the scattering hypothesis in thin films and describes experimental results for both previous investigations and also for the current work on CuAlMo films.

2. Theory

The scattering hypothesis assumes that Mathiessen's [5] rule can be applied so that all contributions to the film resistivity, ρ_f, can be added together as follows:

$$\rho_f = \rho_0 + \rho_{ss} + \rho_{gr} + \rho_{sr} \quad (1)$$

Where ρ_0 is the resistivity of a film of infinite thickness (the bulk material) manufactured under the same conditions and having the same density of defects, and ρ_{ss}, ρ_{gr} and ρ_{sr} are additional contributions to the resistivity from surface scattering, grain boundary scattering and surface roughness scattering respectively.

If the film thickness is approaching the value of the electron MFP, then film surface and film to substrate interface scattering must be considered. In the Fuchs-Sondheimer (FS) model [6, 9] for a continuous single crystalline film, the specularity co-efficient, p, is used to describe the fraction of incident electrons that are specularly scattered at both the film surface and the film to substrate interface and is independent of incident angle, electron energy and surface roughness. Values of p range from 0 to 1, with a low p corresponding to a high resistivity. According to this theory the increase in resistivity of the film due to surface and interface scattering can be calculated to good approximation by:

$$\rho_f = \rho_0 \left[1 + \frac{3\lambda}{8d}(1-p) \right] \quad (2)$$

Where ρ_0 is as defined above, λ is the corresponding MFP of the of the conduction electrons, d is the film thickness and p is the Fuchs scattering parameter.

There have been numerous studies considering the effects of surface scattering on the electrical resistivity of thin films [10-19]. For example, the FS model in equation *(2)* has been shown to give a good fit to experimental data for Cu films of thickness d > 40 nm with p = 0.05 [10]. This low value of p indicates that diffuse scattering of the electrons at the film interfaces is the predominant conduction mechanism, responsible for the resistance increase in this thickness range, and is consistent with

discontinuous film morphology. For Cu films with thickness d < 40 nm the data did not fit the model with any degree of accuracy and additional scattering contributions must be considered.

As the FS model is based upon a single crystal it does not account for grain boundary scattering in polycrystalline films. The quantum effects of grain diameter and grain boundary reflection coefficient were studied by Mayadas and Shatzkes (MS) [7]. The MS model describes a film that represents the grain boundaries as parallel partially reflecting planes, perpendicular to both the electric field and the plane of the sample and placed an average distance, D, apart:

$$\rho_f = \frac{\rho_0}{3}\left[\frac{1}{3} - \frac{1}{2}\alpha + \alpha^2 - \alpha^3 \ln\left(1 + \frac{1}{\alpha}\right)\right]^{-1} \qquad (3)$$

$$\alpha = \frac{\lambda}{D}\frac{R}{1-R}$$

Where D is the average in-plane grain size and R is the grain boundary reflection coefficient. If R = 1, electrons are confined to individual grains as they are reflected back at all surfaces. Mayadas and Shatzkes found values of R to be 0.17 and 0.24 for Al and Cu respectively and grain size, D, was proportional to film thickness, d, ($\lambda/D \; \alpha \; \lambda/d$) and therefore from equation *(3)*, α is also a function of film thickness.

Again there have been many reviews concerning the additional effects of grain boundary scattering on the electrical resistivity of thin films [13-27]. The MS model has been shown to give a good match to experimental data for Cu films of thickness d ~ 20-40 nm when p = 0.05, R = 0.24 and λ/D = 0.3 λ/d [10]. However, for d < 20 nm experimental values still lie above the values predicted by the model. This phenomenon is due the surface roughness effect which must be taken into account for very thin films. The film can no longer be regarded as a homogeneous layer of constant thickness and must be considered to have a thickness which varies around a mean value i.e. a surface roughness. Hence areas of the film which are thinner than others will contribute to an increase in resistivity with increased weighting.

A model that includes the effect of surface roughness in addition to the influence of surface and interface scattering on the resistivity of thin metal films was proposed by Namba [8]. This model is widely referred to as the Fuchs-Namba (FN) model [26-29] and considers the film surface to consist of sinusoidal undulations with irregular indentations. A simplified version of the model can be written as follows, where h is the peak to valley height of the sinusoidal roughness.

$$\rho_f = \rho_0 \left[1 - \left(\frac{h}{d} \right)^2 \right]^{-\frac{1}{2}} + \rho_0 \frac{3\lambda}{8d} (1 - \rho) \left[1 - \left(\frac{h}{d} \right)^2 \right]^{-\frac{3}{2}} \quad (4)$$

The best fit of the FN model for the Cu film discussed earlier is achieved when p = 0.05 and h = 10.3 nm [10]. By including the effects of surface roughness, the model reliably fits the experimental results for resistivity across the full thickness range. However when the value of h was decreased to its true value of 3.5 nm, as measured by AFM, the model fits the resistivity in the high thickness regime but is lower by a factor of approximately four for the lower thickness films. As expected this result indicates that the effect of surface roughness of the copper films decreases with increasing thickness.

3. Experimental Details

All CuAlMo film samples used for conduction studies were prepared on borosilicate glass slides which were ultrasonically cleaned in acetone prior to insertion into the deposition plant. The films were sputtered from a CuAlMo 69/24/7 wt.% target using a Circuit Processing Apparatus 900 (CPA) load locked deposition plant which had been modified to give fully automatic control. All films were deposited at the previously optimised cathode power and sputtering pressure of 1000 W and 0.3 Pa, respectively [1]. No intentional substrate heating was used but under the above conditions a maximum substrate temperature of 325°C could be reached.

Prior to each experimental run the plant was conditioned to improve accuracy. This process has been previously discussed [1] and involved evacuating the plant to a base pressure of 1.33×10^{-5} Pa, before taking a footprint analysis of the gases present in the chamber using a residual gas analyser (RGA), type MKS e-vision Mass Spectrometer, coupled with RGA Data Recall software. For each run this was compared to a control footprint for the plant, to check for any abnormalities. Once the base pressure was satisfactory, the CuAlMo target was pre-sputtered for 30 min under the required experimental conditions, to remove contaminations from the target surface and stabilise the magnetron discharge parameters.

The deposition rate of the CuAlMo film was determined by sputtering samples for a range of times and then measuring the film thickness using an FEI Quanta 200, Scanning Electron Microscope (SEM). A typical plot of sputtering time vs. film thickness, d, is shown in Fig 1. As expected the deposition rate was linear and was determined to have an average value of 190 nm/min.

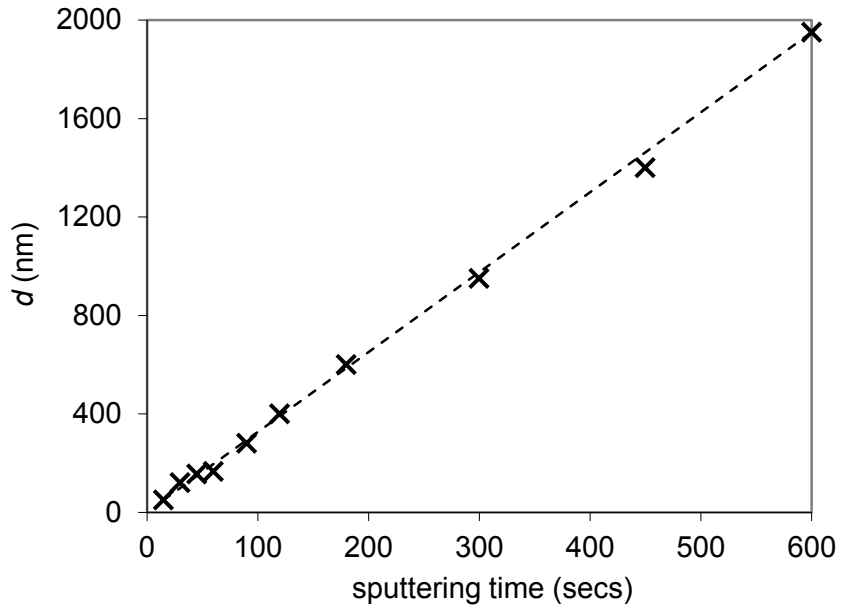

Fig. 1 – Film thickness vs. sputtering time for the CuAlMo films

The resistance of the growing film was measured during deposition using a simplified version of the setup described by Barnet et al, suitable for measurements without a substrate bias [30]. The setup is illustrated in Fig 2 and consists of a four terminal resistance measurement, where the voltage over the film is measured directly and the current is measured indirectly by measuring the voltage across the 50Ω resistor in series with the film, thus eliminating the effects of contact resistance.

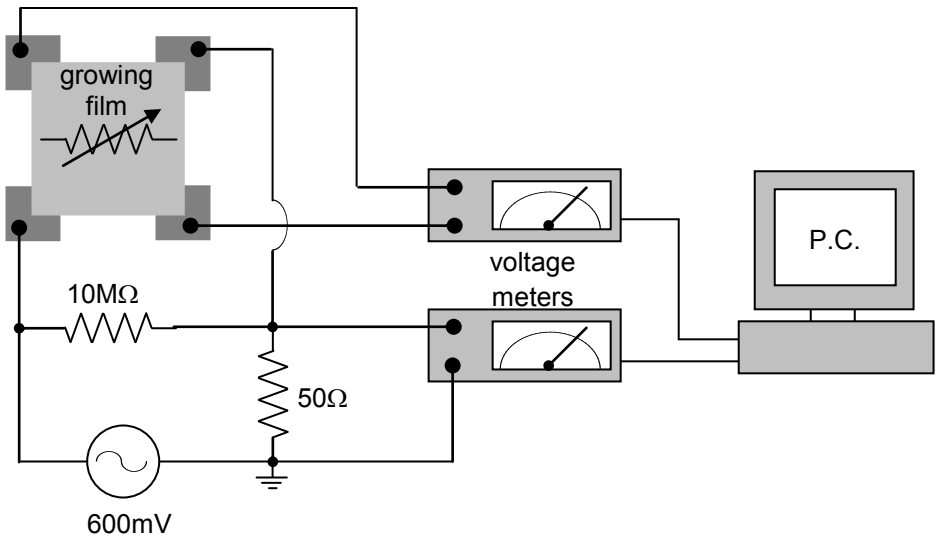

Fig. 2 – Schematic illustration of the in-situ resistance measurement setup [30].

To permit good electrical connection to the film, four thick termination pads were sputtered from Ti/Pd prior to measurement, leaving a square of uncoated substrate onto which the CuAlMo film was deposited. The measured sheet resistance of the termination pads was found to be less than 0.01 Ω/□, which was around two orders of magnitude less than the lowest value measured for the CuAlMo films. Therefore the resistance contribution of the terminations could be ignored and the pads assumed to be equipotential surfaces [12].

The resistance data, R, from the growing film was collected at a rate of 5 times per second by a PC which was interfaced with the measuring equipment. During deposition, the termination pads and connecting wires were shielded from the flux of the plasma by a thin mask of alumina, thus restricting film growth to the exposed square of substrate beneath [31].

Following deposition, the length, l, and width, w, of the film square were accurately measured using a Nikon measurescope MM-22 and the thickness, d, of the film was confirmed to be in good agreement with that reported in Fig 1. The resistivity of the film, p_f, was then calculated as follows:

$$\rho_f = \frac{Rdw}{l} \tag{5}$$

After completion of the in situ resistance measurments, a series of relatively thick CuAlMo films exhibiting bulk conductivity were grown for temperature dependance of resistivity measurements. Following deposition the films were annealed at 430 ˚C for 3 hours in air environment to stabilise the structure, before being protected with two 20-25 μm thick layers of heat curable epoxy protection. Once encapsulated, the temperature dependance of resistance of a sample of 10 of these films was measured across an extended temperature range of -55 to +125 ºC. The resistance measurements were carried out in an Associated Testing Laboratories, Type SLHU-1-LC temperature cycling chamber, using a combination of CO_2 gas and electric heaters to achieve the required test temperature. The temperature was adjusted in 5 ºC increments starting at +25 ºC and decreasing to -55 ºC and then

increasing to +125 ºC before finally decreasing back to +25 ºC, with a 5 min soak at each point. Reported resistance data are the average of the ten CuAlMo films, each measured three times at every temperature increment.

Structural images of the CuAlMo films following deposition and annealing were captured using the FEI Quanta 200 SEM described earlier and x-ray diffraction (XRD) patterns were collected using a Siemens D5000 diffractometer with Cu Kα radiation at 40 kV and 40 mA, with a scanning speed of 0.01 °/s.

4. Results and Discussion

The resistivity of the film, p_f, throughout its growth, as calculated using equation *(5)* is plotted in Fig 3. The resistivity of the film decreases rapidly in the first 20 nm of growth, from approximately 600 μΩcm at 7 nm to 125 μΩcm at 20 nm, during the transition from an island to a continuous film. After this point the reduction is more gradual and at approximately 200 nm the curve flattens off to a value of around 90 μΩcm, indicating the bulk resistivity, p_0. This figure is in good agreement with the as grown resistivity values previously reported for CuAlMo films [32].

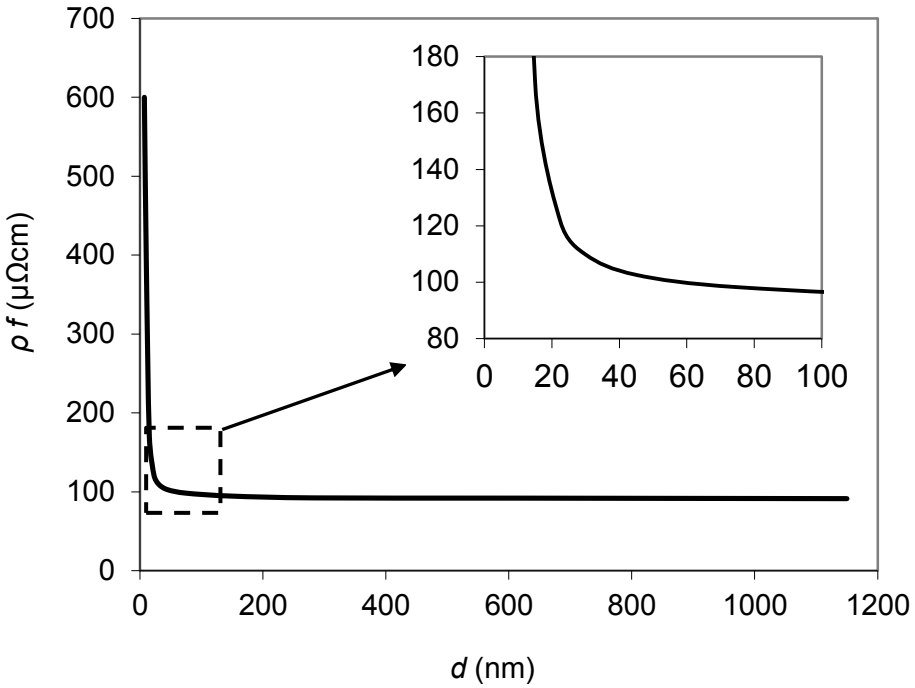

Fig. 3 – Film resistivity as a function of thickness for the CuAlMo films.

For comparison of the experimental results with the theoretical models discussed in section 2, it is convenient to rearrange the Fuchs' equation *(2)* as follows:

$$\rho_f d = \rho_0 \left[d + \frac{3\lambda}{8}(1-p) \right] \qquad (6)$$

It then follows that the graph of dependence $\rho f(d)$ plotted in the coordinates d, $\rho_f d$ will be given by a straight line of slope, ρ_0, and intercept, $\rho_0(3/8)\lambda(1 - p)$. As the specularity co-efficient, p, is not very sensitive to range of values $d/\lambda \pi 1$ used to generate the straight line, no conclusion concerning its magnitude can be drawn from the graph of equation *(6)* and its value can be taken as zero. Thus it is possible to determine the values of ρ_0 and λ from the experimental data.

Fig 4 shows the resistivity data obtained for the CuAlMo films plotted in d vs $\rho f(d)$ coordinates. The values of the bulk resistivity, ρ_0, and MFP, λ, were determined from the graph to be 91.2 μΩcm and 15.7 nm respectively. This theoretical value of ρ_0 is in good agreement with the experimental result for films in the high thickness regime presented in Fig 3. As there has been no previous study undertaken on the CuAlMo system it is difficult to assess the accuracy of the calculated value of λ, however it is interesting to note that previous conduction studies on thin films of Cu and Al have yielded typical values of 39 nm and 18 nm respectively [13]. However when the Cu film was alloyed with 0.5 at.% Al the value of λ was suggested to be <10 nm [14].

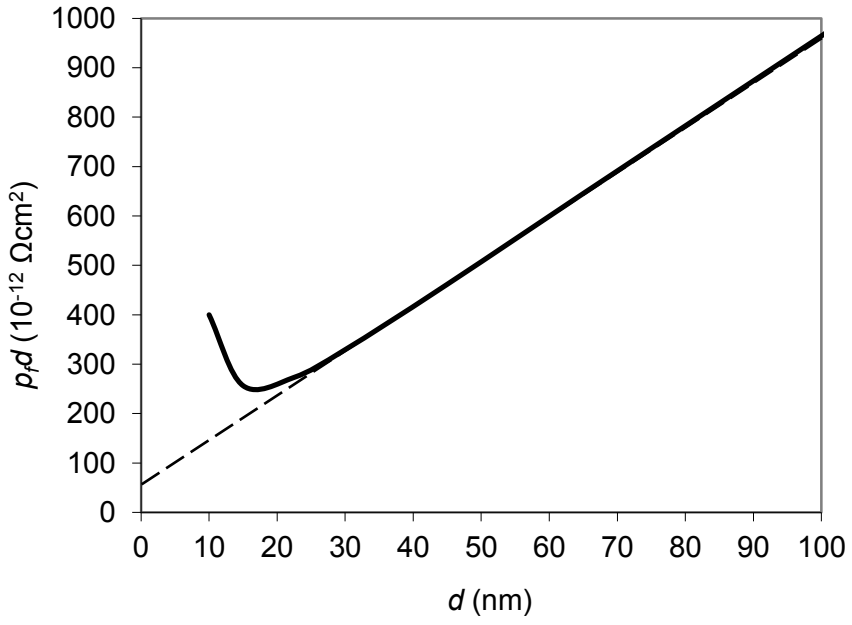

Fig. 4 – Size dependence of the magnitude of pfd on the thickness, d, for the CuAlMo films

To model the increase in ρ_f over ρ_0 with decreasing film thickness it is convenient to plot the ratio of $\rho f/\rho_0$ vs d. Fig 5 shows the experimental resistivity data plotted in these co-ordinates for d < 100 nm with lines fitted for the FS model given in equation *(2)* for different values of the specularity parameter, p.

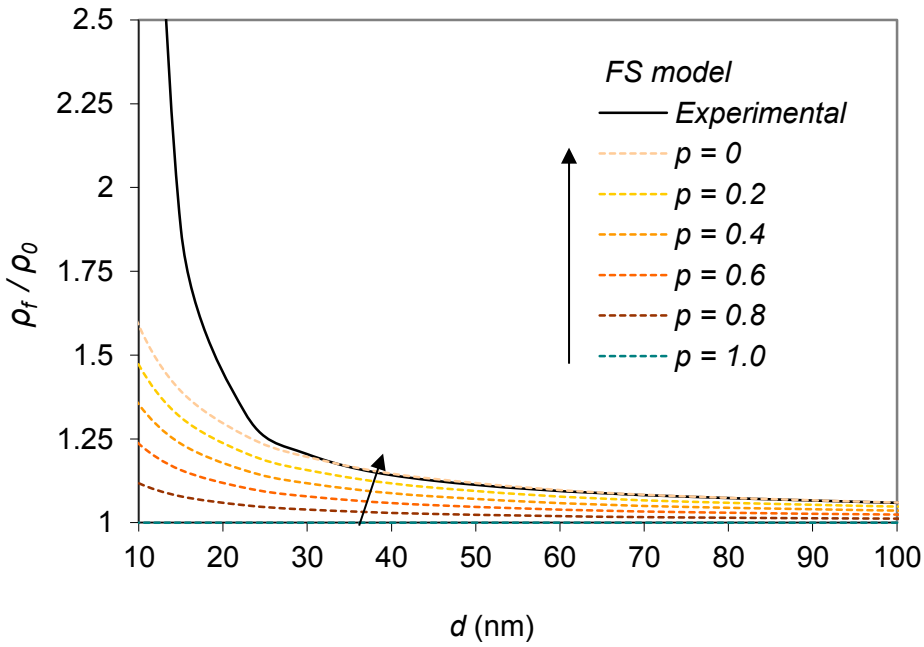

Fig. 5 - The Fuchs-Sonheimer (FS) model fits to the CuAlMo film resistivity data with various surface scattering specularity coefficients, p.

.

For values of d >40 nm the best match between the experimental data and theoretical model is achieved when p <0.05. This result suggests that diffuse scattering of the conduction electrons at the two surfaces is the predominant mechanism for the increase in ρ_f in this thickness range. The calculated resistivity does not match the data for d <35 nm and other mechanisms must be considered.

Fig 6 shows the curves calculated from the MS model given in equation *(3)* with p = 0.05. When R = 0.22 and λ/D = 0.85λ/d a good fit was found with the experimental results for d ~ 25-40 nm. However, for d <25 nm the calculated values are still low compared to experimental results.

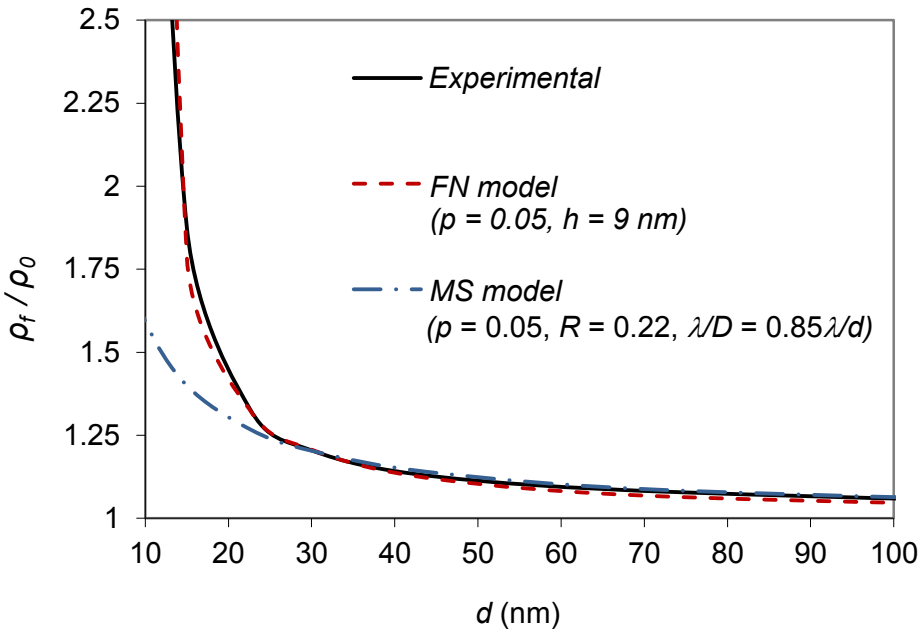

Fig. 6 – The Mayadas & Shatzkes (MS) and Fuchs-Namba (FN) model fits to the CuAlMo film resistivity data with p = 0.05, R = 0.22, λ/D = 0.85λ/d and h = 9nm.

The results of the FN model given in equation *(4)* are also plotted in Fig 6. By incorporating the effects of surface roughness in addition to surface and interface scattering, excellent correlation between the model and the experimental result is achieved. The best fit was attained with values of p = 0.05 and h = 9 nm, which is in good agreement with previous results reported using the Namba model [10].

Following determination of the dominant conduction mechanisms, a series of CuAlMo films exhibiting bulk resistivity were grown in the the thickness range 730-1060 nm to study their temperature dependence of resistivity.

The as grown resistivity of the films was ~91 μΩcm and decreased to ~69 μΩcm following annealing at 430 ˚C fo 3 hours in air environment. This decrease in resistivity following annealing can be related to an increase in grain size and consequently a decrease in grain boundaries, leading to an increase in the conductivity of the films due to the reduction in charge-carrier scattering by grain boundaries [33] and is supported by the SEM micrographs of surface morphology of the films in Fig 7. The average crystallite size, as determined from variation in the full

width half maximum (FWHM) of the (330) plane of the γ_2 (Cu_9Al_4) phase and calculated using the Scherrer equation [34], increases from 14 nm for the as grown films to 24 nm following annealing.

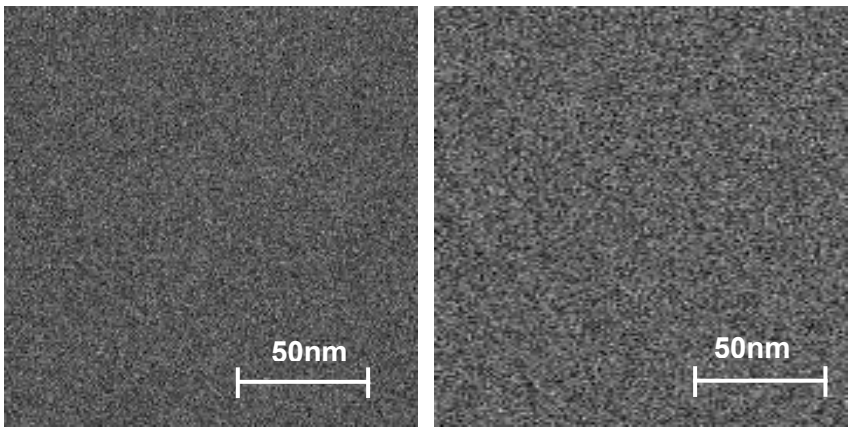

(a) (b)

Fig. 7 – SEM micrographs of CuAlMo films on glass substrates (a) as grown, (b) annealed at 430 ˚C for 3 hours in air.

Fig 8 shows the temperature dependence of resistance, *Rf*, for the annealed CuAlMo films measured across the temperature range of -55 to +125 ºC. The mean resistance of the films decreases with both negative and positive changes in temperature.

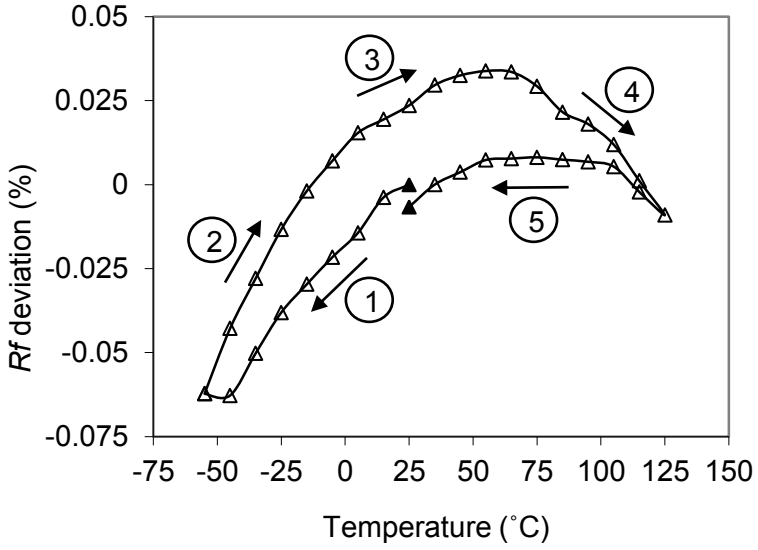

Fig. 8 – Temperature dependence of resistance *for CuAlMo films grown on glass substrates and annealed at 430 ˚C for 3 hours in air.*

Two important properties which can be established from the plot of *T* vs *Rf* in Fig 8 are the irreversibility of resistance and the temperature co-efficient of resistance (TCR) of the films. For both of these parameters it is usual to specify an upper and lower temperature result with reference to room temperature (25 ˚C), as reported in Table 1.

Table 1 – Mean irreversibility of resistance and TCR results for CuAlMo films grown on glass substrates and annealed at 430 ˚C for 3 hours in air.

Test	Temperature range (ºC)	Result
Irreversibility of resistance (%)	+25 / -55 / +25	0.024
	+25 / +125 / +25	-0.030
TCR (ppm/ºC)	+25 to -55	-12 to -2
	+25 to +125	-8 to 0

The irreversibility of resistance for the films was less than 0.03 % following subjection to both negative and positive temperatures of -55 and +125 ºC and the TCR was less than 15 ppm/ºC, thus highlighting the potential application of the CuAlMo material to produce highly stable low resistivity thin film resistors.

5. Conclusions

By theoretically modelling the evolution of resistivity during the growth of the CuAlMo films under optimised sputtering conditions it has been possible to gain an insight into the types of electrical conduction involved with increasing film thickness. The transition between dominant mechanisms is shown in Fig 9.

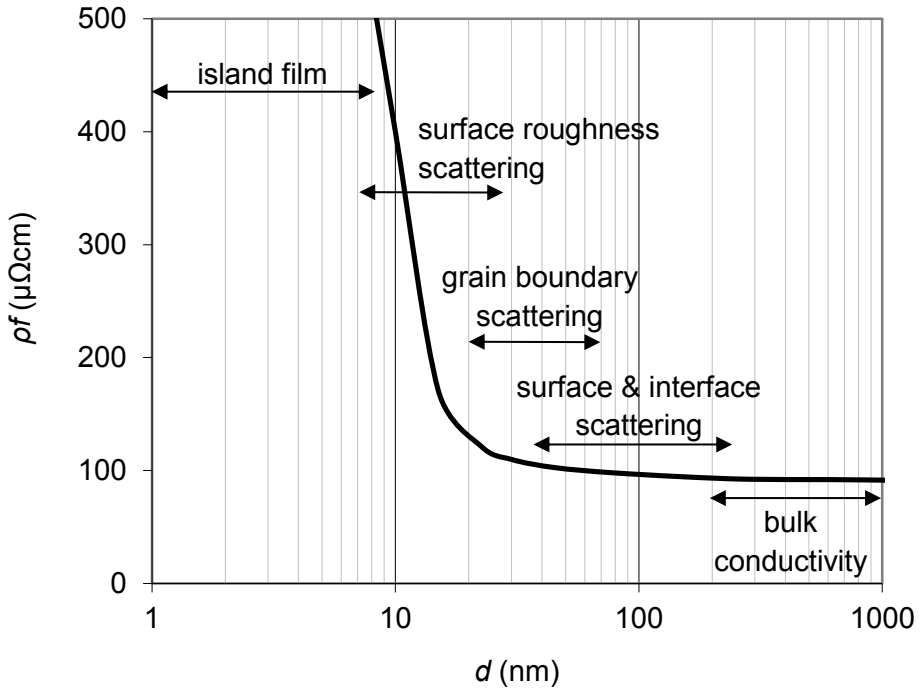

Fig. 9 – Dominant conduction mechanisms with increasing thickness of CuAlMo films

For film thicknesses, d ~ <10 nm the CuAlMo film is in a discontinuous state and consists of a network of isolated islands with infinite resistivity. As these islands start to grow and coalesce, a continuous film is formed, which is marked by the rapid increase in conductivity for d = 10-25 nm. Electrical resistivity in this thickness range was assumed to be a function of the film surface roughness and was suitably described using Namba's model which assumes the sample surface to consist of sinusoidal undulations with irregular indentations.

As the CuAlMo film grows further its resistivity begins to level off towards its bulk value and the effects of surface roughness are decreased. In this thickness range the effects of grain boundary and surface scattering of electrons become the dominant mechanisms. For d = 25-40 nm the experimental data was most accurately

fitted using the Mayadas and Shatkes model which accounts for grain boundary scattering of the conduction electrons. For d >40 nm, the thickness of the film was found to be the controlling factor and the Fuchs-Sonheimer model was used to fit the experimental data, with diffuse scattering of the conduction electrons occurring at the film's two surfaces.

By combining the Fuchs and Namba models a suitable correlation between theoretical and experimental resistivity can be achieved across the full film thickness range of 10-1000 nm. For d ~ >200 nm the resistivity curve flattens off completely and bulk conductivity is assumed. The calculated bulk resistivity of 91.2 μΩcm is in good agreement with earlier experimentation for as-grown CuAlMo films.

As one of the primary objectives of this work is to attain films of low sheet resistance, the vast majority of CuAlMo films under investigation will be in the thickness range d >200 nm. Hence, from the work in this paper it can be concluded that bulk conductivity will be the dominating conduction mechanism in these films. The irreversibility of resistance for films in this thickness range beyond 200 nm was shown to be less than 0.03 % following subjection to temperature cycles of -55 and +125 ºC and the temperature co-efficient of resistance was less than ±15 ppm/ºC. These results are in good agreement with previous figures reported for CuAlMo films [1] and further demonstrate their suitability for the fabrication of precision thin film resistor devices.

References

[1] M. Birkett, R. Penlington, C. Wan, G. Zoppi, Thin Solid Films. 540 (2013) 235-241.

[2] M. Birkett, R. Penlington, IEEE. T. Compon. Pack. A. 3 (2013) 523-529.

[3] M. Birkett, R. Penlington, J. Electron. Mater. 41 (2013) 2169-2177.

[4] D. Shih, P. Ficalora, J. Vac. Sci. Technol. A. 2 (1984) 225-230.

[5] G. Zhigal'skii, B. Jones, Electrocomponent Science Monographs – The Physical Properties of Thin Metal Films, Taylor and Francis, New York, 2003.

[6] K. Fuchs and H. Wills, P. Camb. Philos. Soc. 34 (1938) 100-108.

[7] A. Mayadas, M. Shatzkes, Phys. Rev. 1 (1970) 1382-1389.

[8] Y. Namba, Jap. J. Appl. Phys. 9(11) (1970) 1326-1329.

[9] E. Sondheimer, Adv. Phys. 1(1) (1952) 1-42.

[10] H. Liu, Y. Zhao, G. Ramanath, S. Murarka, G. Wang, Thin Solid Films. 384 (2001) 151-156.

[11] D. Campbell, A. Morley, Rep. Prog. Phys. 34 (1971) 283-368.

[12] J.S. Agustsson, U.B. Arnalds, A.S. Ingason, K.B. Gylfason, K. Johnsen, S. Olafsson, J.T. Gudmundsson, Appl. Surf. Sci. 254 (2008) 7356-7360.

[13] M. Sinha, S. Mukherjee, B. Pathak, R. Paul, P. Barhai, Thin Solid Films. 515 (2006) 1753-1757.

[14] E. Lee, N. Truong, B. Prater, J. Kardokus, Semiconductor International (2006) - 7/1/2006.

[15] C. Tellier, A. Tosser, Electrocomp. Sci. Tech. 6 (1980) 91-92.

[16] V. Das, P. Ganesan, Semicond. Sci. Tech. 12 (1997) 195-202.

[17] J. de Vries, F. den Broeder, J. Phys. F. Met. Phys. 18 (1988) 2635-2647.

[18] W. Zhang, S. Brongersma, O. Richard, B. Brijs, R. Palmans, L. Froyen, K. Maex, Microelectron. Eng. 76 (2004) 146-152.

[19] K. Gylfason, A. Ingason, J. Augustsson, S. Olafsson, K. Johnsen, J. Gudmundsson, Thin Solid Films. 515 (2006) 583-586.

[20] E. Barnat, D. Nagakura, P. Wang, T. Lu, J. Appl. Phys. 91 (2002) 1667-1672.

[21] A. Tosser, C. Tellier, J. Launey, Vacuum. 27(4) (1977) 335-338.

[22] F. Magnus, A.S. Ingason, S. Olafsson, J.T. Gudmundsson, Thin Solid Films. 519 (2011) 5861-5867.

[23] H. Van Bui, A.Y. Kovalgin, R.A.M. Wolters, Appl. Surf. Sci. 269 (2013) 45-49.

[24] S. Bahamondes, S. Donoso, A. Ibanez-Landeta, M. Flores, S. Bahamondes, S. Donoso, A. Ibanez-Landeta, M. Flores, Appl. Surf. Sci. 332 (2015) 694-698.

[25] M. Avrekh, O.R. Monteiro, I.G. Brown, Appl. Surf. Sci. 158 (2000) 217-222.

[26] U. Jacob, J. Vancea, H. Hoffmann, J. Phys-Condens. Mat. 1 (1989) 9867-9873.

[27] D. Dayal, P. Rudolf, P. Wissmann, Thin Solid Films. 79 (1981) 193-199.

[28] W. Prater, E. Allen, J. Appl. Phys. 97 (2005) 093301.

[29] S. Shayestehaminzadeh, T.K. Tryggvason, F. Magnus, S. Olafssona, J.T. Gudmundsson, Thin Solid Films. 549 (2013) 199-203.

[30] E. Barnet, D. Nagakura, T. Lu, Rev. Sci. Instrum. 74(7) (2003) 3385.

[31] U. B. Arnalds, J.S. Agustsson, A. S. Ingason. A. K. Eriksson, K. B. Gylfason, J. T. Gudmundsson, S. Olafsson, Rev. Sci. Instrum. 78(10) (2007) 3901.

[32] M. Birkett, J. Brooker, R. Penlington, A. Wilson, K. Tan, IET. Sci. Meas. Technol. 2(5) (2008) 304-309.

[33] Y. Kwon, N. Kim, G. Choi, W. Lee, Y. Seo, J. Park, Microelectron Eng. 82 (2005) 314.

[34] B. Cullity, Elements of x-ray diffraction, Addison-Wesley Publishing Company, Boston, 1978.